Numerical Assessment of the Contribution of Liquefaction and Directivity on the Seismic Displacement of a Quay Wall during the 2014 Cephalonia, Greece, Earthquakes

George Zalachoris, Ph.D.[1]; Dimitrios Zekkos, Ph.D., P.E., M.ASCE[2];
Adda Athanasopoulos-Zekkos, Ph.D., M.ASCE[3]; Nikos Gerolymos, Ph.D., M.ASCE[4];
and Yiannis Tsiapas, Ph.D.[5]

[1]Geotechnical Engineering Consultant, ElxisGroup, Athens, Greece.
Email: gzalachoris@elxisgroup.com
[2]Associate Professor, Dept. of Civil and Environmental Engineering, Univ. of California at Berkeley, Berkeley, CA. Email: zekkos@geoengineer.org
[3]Assistant Professor, Dept. of Civil and Environmental Engineering, Univ. of California at Berkeley, Berkeley, CA. Email: adda.zekkos@berkeley.edu
[4]Associate Professor, School of Civil Engineering, National Technical Univ. of Athens, Athens, Greece. Email: gerolymo@mail.ntua.gr
[5]Research Associate, School of Civil Engineering, National Technical Univ. of Athens, Athens, Greece. Email: ioannis.tsiapas@gmail.com

ABSTRACT

During the Cephalonia, Greece, 2014 earthquake sequence (M_w=6.1 and M_w=6.0), the quay walls in the port of Lixouri, Cephalonia, displaced laterally up to 1.5 m, while liquefaction of the gravelly port earthfills resulted in the manifestation of ground cracking and coarse-grained ejecta. To evaluate the seismic performance of the Lixouri port quay walls, numerical analyses using the finite difference method were performed at the location where the largest horizontal displacements were observed and the results are compared to the observed response. Three commonly used constitutive models (PM4SAND, UBCSAND, and URS/ROTH), informed by data from site investigation efforts (Dynamic Penetration Test, DPT, and Multichannel Analysis of Surface Waves, MASW), were considered for the simulation of the behavior of the liquefiable earthfills. The results of the numerical analyses indicate that liquefaction of the earthfills significantly contributed to the total lateral deformations of the quay walls; without liquefaction, the computed horizontal displacements are only approximately 30% of the observed lateral spreading when liquefaction occurs. Overall, the numerical analyses using best-estimate input parameters for the PM4SAND and UBCSAND models significantly under-predict the observed response, while the computed horizontal displacements are approximately 25% smaller than observed when the URS/ROTH model is used. The difference between model predictions can be partially attributed to the incorporation of residual shear strength once liquefaction is triggered when using the URS/ROTH model. Finally, the results of the numerical analyses show the strong influence of the pulse-like characteristics as well as the polarization of the input motion, indicating that forward directivity also significantly contributed to the observed response.

GRAVEL LIQUEFACTION AT LIXOURI PORT DURING THE 2014 CEPHALONIA EARTHQUAKES

Cephalonia island, located west of mainland Greece in the Ionian Sea, is characterized by a long history of seismic activity. In early 2014, an earthquake doublet occurred near Cephalonia.

The two main seismic events, which occurred on January 26 and February 3, had magnitudes of M_w=6.1 and M_w=6.0, respectively. The earthquakes caused extensive ground failures, including soil liquefaction, at the port town of Lixouri (GEER, 2014). Based on the findings of the post-event reconnaissance, the second event (February 3, 2014) was significantly more damaging than the first (January 26, 2014), something that has been partially attributed to a forward rupture directivity effect during the second event (Garini et al., 2017).

In this study, the soil liquefaction that was observed at the port of Lixouri is investigated. Liquefaction caused extensive ground cracking and the manifestation of soil ejecta at the ground surface, while also contributing to the lateral ground displacements of the port quay walls in Lixouri ranging from a few centimeters to more than a meter. Calibrated using in-situ investigation data, numerical models of the quay walls are developed and described in detail. The results of the numerical analyses are compared with the observed responses and insights on the physical mechanisms behind the quay wall behavior during the seismic loading, are provided.

STRONG GROUND MOTIONS AND PERFORMANCE OF QUAY WALLS

The two Cephalonia 2014 seismic events were recorded by several permanent strong motion stations of the Hellenic Unified Seismic Network (HUSN). The present study focuses on the ground motions recorded at the seismic station located in Lixouri (LXRB). LXRB station recorded larger peak ground accelerations (PGA) during the February 3 earthquake (0.67g, for the East-West direction). In Figure 1, the acceleration time histories and the corresponding 5% damped acceleration response spectra for the February 3 record in LXRB, are presented. The ground motion at Lixouri (LXRB) shows a pulse-like characteristic in its East-West (EW) component (Figure 1a), which translates into significant spectral accelerations (~1.6g) at long periods (T≈1.3s) (Figure 1b). Such observations are consistent with forward rupture directivity.

The 2014 earthquake sequence resulted in manifestation of coarse-grained soil ejecta at several locations near and along the port of Lixouri, where the grain size of ejecta had a maximum diameter of 3 cm (Athanasopoulos-Zekkos et al., 2019). To evaluate the performance of the quay walls at Lixouri, Athanasopoulos et al. (2019) documented the cumulative horizontal wall displacements along 8 transects with orientation perpendicular to the quay wall front. These displacements are a combination of the: i) liquefaction-induced lateral spreading, and ii) translational and rotational movement of the quay walls due to the dynamic excitation.

The port of Lixouri (Figure 2a) is characterized by a North-South direction of its main waterfront (main Pier). The height of the quay walls is variable (2.6 m to 7.6 m), while the land area behind the walls consists of reclamation fills placed using building debris (Geoconsult Ltd, 2016). The distance of the Lixouri port from the causative fault of the February 3 earthquake is approximately 2 km, while the LXRB station is located at a distance of ~200 m inland (Figure 2a). Even though manifestation of liquefaction was reported following both earthquakes, most of the lateral movement of the quay walls was a result of the second event.

Athanasopoulos et al. (2019) reported horizontal displacements at the back face of the walls ranging from 4.3 cm to 152 cm. Most of the displacements occurred within the first 30 m from the waterfront. To assess the observed response, the present work focuses on the transect that exhibited the largest displacements during the 2014 Cephalonia earthquake sequence, as documented by Athanasopoulos et al. (2019). Figure 2a shows the selected transect (TS-7, hereafter), and also depicts a characteristic photo of the damaged quay wall. Figure 2b presents the cumulative horizontal displacements along the first 30 m behind the quay wall face at the selected location.

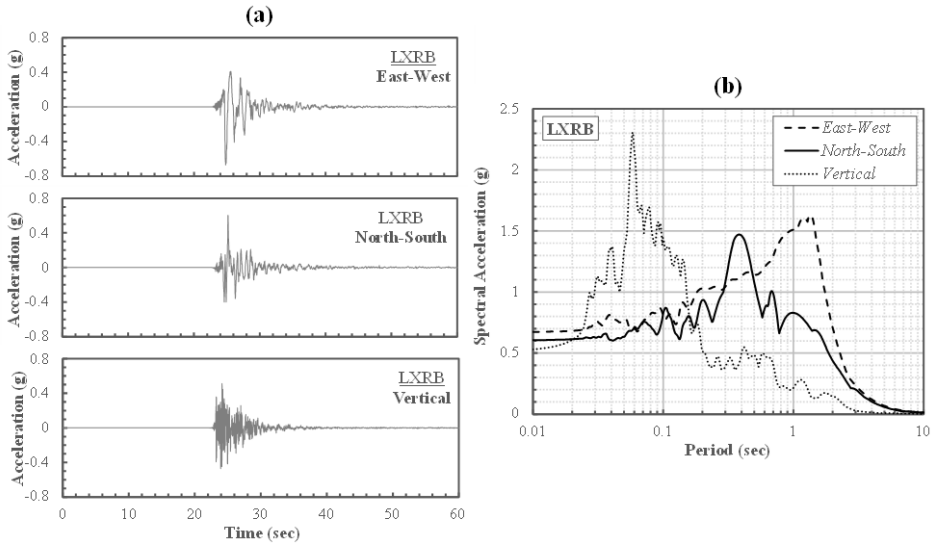

Figure 1. a) three component strong motion recordings, and b) associated 5%-damped acceleration response spectra at Lixouri (LXRB) seismic station (February 3 event).

SITE CONDITIONS

Following the 2014 earthquake sequence, a geotechnical site characterization study was performed at the port of Lixouri (Geoconsult Ltd, 2016). This initial site investigation included 11 boreholes and 13 test pits. According to this in-situ investigation, the sea reclamation fill consists of large stones, with diameters ranging from 10 to 60 cm, in a matrix of finer material of gravels, sands and low plasticity silts. The data from the initial in-situ geotechnical investigation (Geoconsult Ltd, 2016) are primarily used for the development of index properties for the native soil and the reclamation fills, as well as for the determination of the quay wall geometry at the selected location in Lixouri port (Figure 2a).

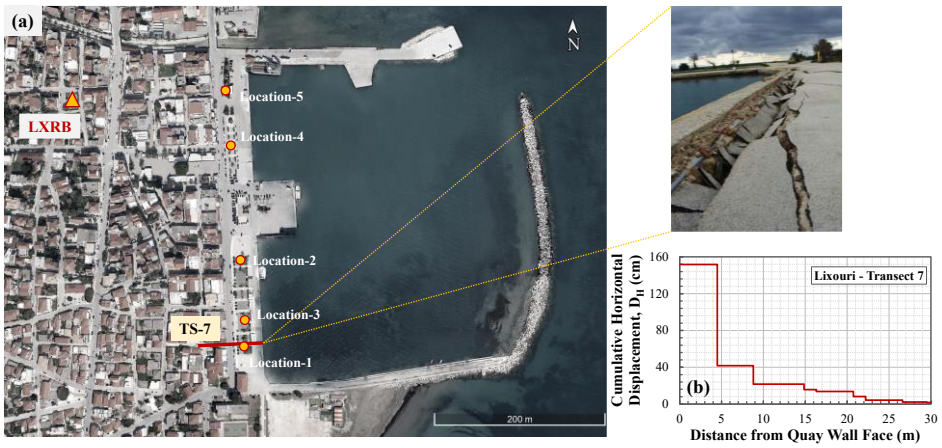

Figure 2. Lixouri port: a) location of strong motion station, selected transect, site investigation location, and photo of observed quay wall damage. Photo from Geotechnical Investigation Report, Geoconsult Ltd., 2016, b) Distribution of measured cumulative lateral spreading displacements along transect TS-7 (Athanasopoulos et al., 2019).

To better constrain the material behavior, Athanasopoulos-Zekkos et al. (2019) further characterized the gravelly reclamation fill at five locations within the port of Lixouri using Dynamic Penetration Testing (DPT), as well as the Multichannel Analysis of Surface Waves (MASW) method. The locations and numbering of these tests are shown in Figure 2a. Dynamic Cone Penetration Tests (DPT) were conducted using the same cone tip described by Cao et al. (2013). DPT was selected by Athanasopoulos-Zekkos et al. (2019) as an alternative to Standard Penetration Testing (SPT) and Cone Penetration Testing (CPT), which can be unreliable in gravelly deposits due to the larger particle sizes involved. To obtain N'_{120}, the measured DPT blow counts were corrected to account for differences in the rig weight and drop height between the test apparatus used and the one described by Cao et al. (2013). Furthermore, Athanasopoulos-Zekkos et al. (2019) performed Multichannel Analysis of Surface Waves (MASW) tests to develop representative shear wave velocity (V_S) profiles. The DPT data were used to develop layering for the V_S profiles based on site stratigraphy and to constrain the forward modeling and generate more refined estimates of V_S.

Using the information collected by the aforementioned site investigation efforts, representative wall geometry and material properties for the selected site in Lixouri port were developed. A schematic that depicts the soil layering, wall geometry, as well as the corresponding N'_{120} and V_S profiles, at the analyzed quay wall location, is presented in Figure 3. The selected wall geometry in Lixouri (TS-7) includes a relatively short, 2-block concrete wall with a height of H=2.6 m. In terms of geologic setting and stratigraphy, the concrete blocks are founded on medium dense to dense sand and gravel, with intercalations of cobles of limestone/sandstone origin. The foundation material is underlain by alluvial deposits consisting of low to medium plasticity clays (CL) of variable thickness, sandy in places, which is characterized by an ash-green to black-green color (Geoconsult Ltd, 2016). The alluvial deposits are underlain by a stiff cohesive formation extending to the maximum investigated depth.

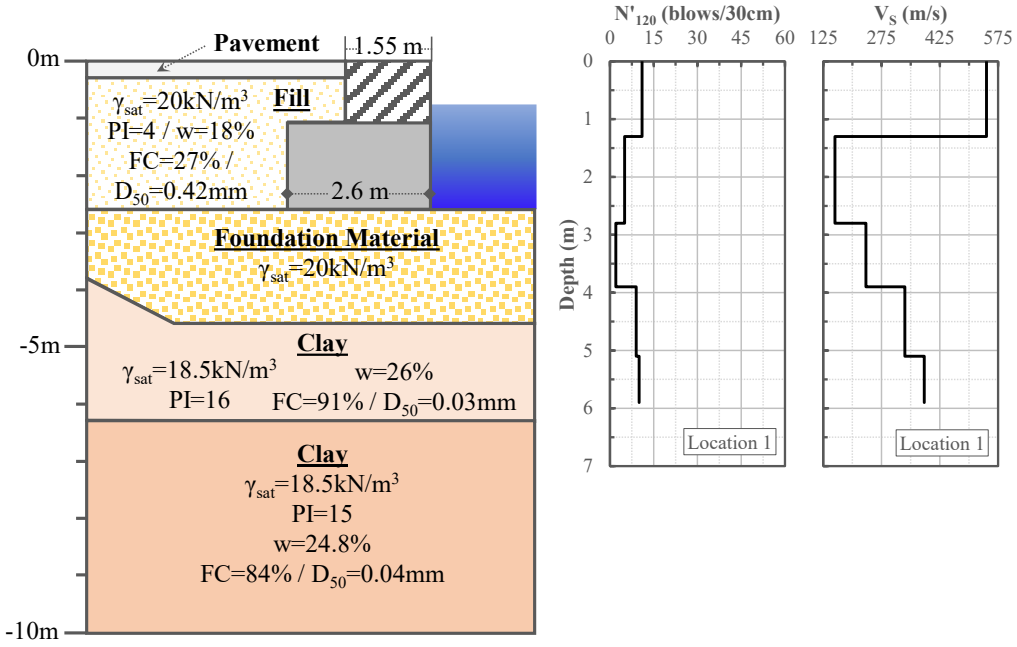

Figure 3. Wall Geometry and data from in-situ site investigation at Lixouri TS-7 wall.

NUMERICAL MODELING OF QUAY WALL DYNAMIC RESPONSE

The available strong ground motion recordings in the vicinity of the ports, the detailed documentation of the observed response of the coastal structural systems, as well as the extensive in-situ investigation data generated, consist of a well-documented case history that can inform the validation of numerical tools. Herein, we use the finite difference method, to computationally simulate the response of the quay wall at the selected location in Lixouri (Figure 2a). The results of these simulations are compared to the field observations (Figure 2b).

For the development of the numerical model, we utilized the two-dimensional, explicit, finite difference software FLAC (Fast Lagrangian Analysis of Continua) v8. (Itasca, 2016). The materials are represented by rectangular zones, which collectively form a grid that is adjusted to model the wall geometry and stratigraphy. The generated model geometry, numerical mesh and the associated idealized stratigraphy for the Lixouri TS-7 wall is illustrated in Figure 4. The grid consists of zones with an average size of approximately 0.45 m × 0.45 m with a maximum aspect ratio of 2:1. To capture a more detailed distribution of accelerations and stresses at regions of interest, denser zoning was generated behind the quay wall.

The planes on which sliding or separation can occur, namely the horizontal or vertical interfaces between the foundation material or the reclamation fill and the concrete blocks, as well as the planes of contact between the stacked wall blocks, are simulated using the interface features available in FLAC. Unglued interfaces (no dilation and no tensile strength) were adopted, with generic values for the normal and shear stiffnesses (10^{10} Pa), and friction angles equal to 30° for the contacts between the concrete blocks, and 0.7·φ (where φ is the effective friction angle of the corresponding soils) for the interfaces between the wall and the soil materials.

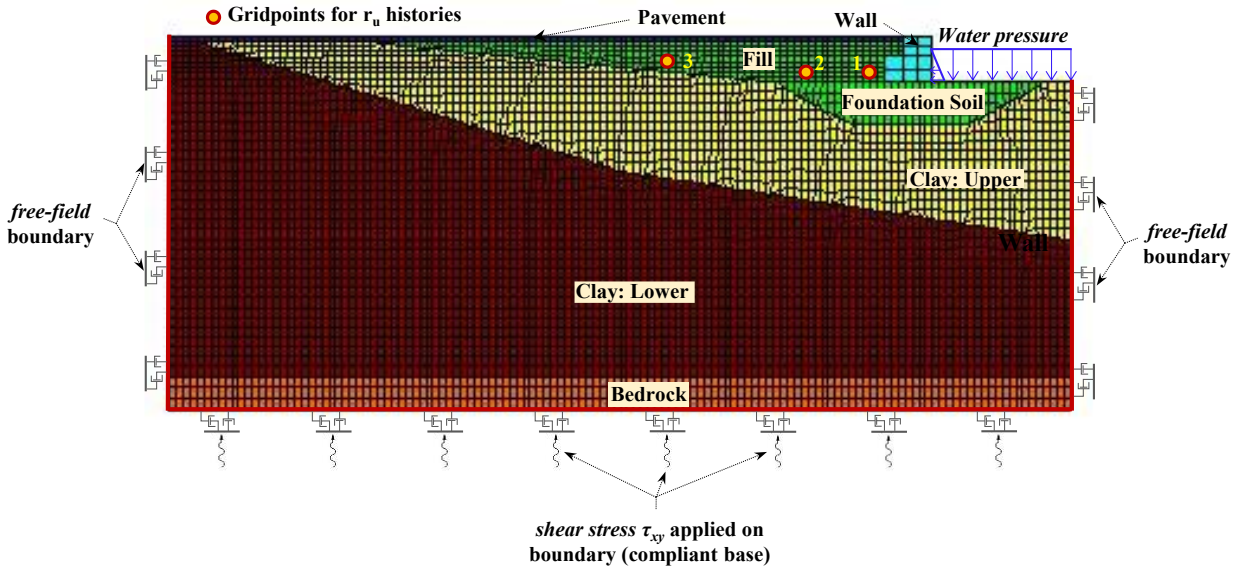

Figure 4. Schematic of FLAC mesh, boundary conditions and application of input motion.

Material model properties were selected for each layer, based on the data from the site investigation efforts (Figure 3). Default curves of hysteretic behavior (G/G_{max}–logγ and D-logγ),

based on the sigmoidal equation with three parameters (sig3), as available in FLAC, were defined for the non-liquefiable materials. An additional mass-and-stiffness proportional Rayleigh damping of ξ_{min} = 1%, anchored at f_{min} = 1 Hz was, also, added to the model. The lateral boundaries are simulated as "free-field" zones, i.e., the boundaries retain their nonreflecting properties (outward waves are absorbed). Finally, all zones below the water table (elevation of -1 m) were considered fully saturated, while the effect of the presence of water at the seaside of the quay wall, was modeled via a mechanical hydrostatic pressure applied on the upper-right horizontal, and vertical, model boundaries. The liquefiable reclamation fill response is simulated using three user-defined constitutive models: i) PM4Sand (version 3.1, Boulanger and Ziotopoulou, 2018), ii) UBCSand (version 904aR, Beaty and Byrne, 2011), and iii) URS/ROTH (Dawson et al., 2001; revised 2018).

For the PM4Sand model, only three parameters need to be specified: the relative density D_R, the contraction rate parameter h_{p0}, and the shear modulus coefficient G_0. Relative density (D_R) is estimated by correlation to SPT $N_{1,60}$ values ($D_R = \sqrt{N_{1,60}/46}$; Idriss and Boulanger, 2008), the coefficient G_0 is obtained by the in-situ shear wave velocity (V_S) measurements, and h_{p0} is used to modify the soil contractiveness and therefore enable calibration of the models to specific values of Cyclic Resistance Ratio (CRR). The UBCSand model has 13 input parameters but includes default calibration values for all parameters based on the specified SPT $N_{1,60}$ value. Model calibration to specific values of CRR is performed by varying the elastic shear stiffness (K_G^e), bulk stiffness (K_b), and plastic shear modulus (K_G^p) parameters. The URS/ROTH model, built around the Mohr Coulomb model, generates pore pressure from shear stress cycles based on the Seed-Idriss cyclic stress approach (Dawson et al., 2001). Once liquefaction is triggered, the material is assigned its residual shear strength. The residual strength of the fills is estimated by empirical relationships between the residual shear strength ratio (S_r/σ'_v) and the SPT equivalent clean-sand, corrected blow count (Boulanger and Idriss, 2011).

Athanasopoulos-Zekkos et al. (2019) showed that liquefaction triggering analyses using the DPT data and recommendations by Cao et al. (2013) are not always consistent with field observations. Accordingly, herein, the obtained DPT N'_{120} blowcounts are converted to equivalent SPT N'_{60} values, and the latter values are used to determine liquefaction triggering. The empirical SPT N'_{60} - DPT N'_{120} correlation proposed by Talbot (2018) was adopted. Talbot (2018) used data from four sites in Idaho, U.S.A., to develop an overall relationship of $N'_{60} \approx 0.75 \times N'_{120}$. It is worthwhile to note that the estimated DPT-equivalent N'_{60} values are similar to the V_S-equivalent SPT values, computed by utilizing the V_S-N_{SPT} correlation developed by Athanasopoulos (1995).

The calibration procedure for PM4Sand and UBCSand involved the variation of h_{p0} for PM4Sand, and K_G^e, K_b, and K_G^p for UBCSand, until the CRR values derived from single element, uniform, cyclic, undrained Direct Simple Shear (DSS) simulations matched the target CRR values for M_w=7.5 and M_w=6.0, computed using the SPT-based liquefaction triggering correlation by Idriss and Boulanger (2008). The material properties of the liquefiable layers, the target CRR values, the calibrated PM4Sand and UBCSand model parameters, as well as the URS/ROTH model parameters are tabulated in Tables 1 and 2.

The dynamic excitation is applied at the bottom model boundary. A compliant base is assumed to minimize the effect of reflected waves, i.e., a quiet (viscous) boundary is assigned along the base of the model, in both the x- and y-directions. The input ground motion is applied as a shear-stress time history, $\tau_{xy}(t)$, along the base (Figure 4), by converting the "Incoming Only" part of the bedrock velocity time history, $V(t)$, using $\tau_{xy}(t) = -2\rho V_S \cdot V(t)$, where,

ρ=dry unit weight of bedrock, and V_S=shear wave velocity of bedrock. The "Incoming Only" bedrock velocity time history in Lixouri (EW component) is obtained via deconvolution analyses (Figure 5).

RESULTS OF NUMERICAL ANALYSES

Using the aforementioned model geometry, input ground motion and best-estimate material properties and calibrated constitutive model parameters, a series of numerical analyses were performed for the selected Lixouri TS-7 quay wall. At first, the resulting deformed shape and contours of the excess pore pressure ratio (r_u) at the end of shaking, are presented in Figure 6a. Moreover, Figure 6b depicts the computed r_u time histories at three selected zones behind the quay wall; one right next to the retaining system (point 1), one at a "free-field" zone, at a distance greater than 20 m from the face of the walls (point 3), and one in a zone in-between (point 2). The results are shown only for the PM4Sand model, used as the baseline case in this study.

Table 1. Properties for the potentially liquefiable layers

Material	in-situ DPT blowcounts N'_{120}	equivalent SPT blowcounts N'_{60}	Shear Wave Velocity V_S (m/s)	Friction Angle φ (deg.)	Target Cyclic Resistance Ratio (M_w=7.5, σ'_v=1atm) $CRR_{M=7.5}$	Target Cyclic Resistance Ratio (M_w=6.0, σ'_v=1atm) $CRR_{M=6.0}$
reclamation fill	5	3.8	155	33	0.105	0.151
foundation soil*	-	5.6	200	32	0.119	0.171

*Note: equivalent SPT blowcounts computed using the V_S-N_{SPT} correlation by Athanasopoulos (1995)

Table 2. Calibrated PM4Sand, UBCSand and URS/ROTH model parameters for the liquefiable layers

PM4Sand				UBCSand			URS/ROTH		
Property		Reclamation Fill	Foundation Soil	Property		Reclamation Fill	Property		Reclamation Fill
Relative Density	D_R (%)	42	47	Shear Modulus Number	k_G^e	403	b-parameter (cyclic strength curve)	b	0.34
Shear Modulus Coefficient	G_0	403	592	Bulk Modulus	k_b	282	Residual Shear Strength Ratio	S_r/σ'_v	0.095
Contraction Rate Parameter	h_{p0}	0.70	0.40	Plastic Shear Modulus	k_G^p	177			
				Failure Ratio	R_f	0.806			

Zones of excess pore pressure buildup (r_u>0.7) are evident in Figure 6a. The largest values of excess pore pressure ratios are observed in the free field (point 3), where r_u approaches unity

within 2-3 sec after the initiation of shaking. However, behind the wall (point 1), lower r_u values are generated. In fact, significant negative excess pore pressure ratios are observed between 5 and 10 sec of the dynamic input (Figure 6b). This can be explained by the effect of the wall movement. As the wall undergoes translational and/or rotational movements, the soil behind it tends to develop negative excess pore pressures and a dilative behavior is triggered. Negative excess pore pressures are developed at point 1 simultaneously with excessive wall movements. Once the rate of the displacements of the concrete blocks is reduced (i.e., at t>10 sec), r_u becomes again highly positive.

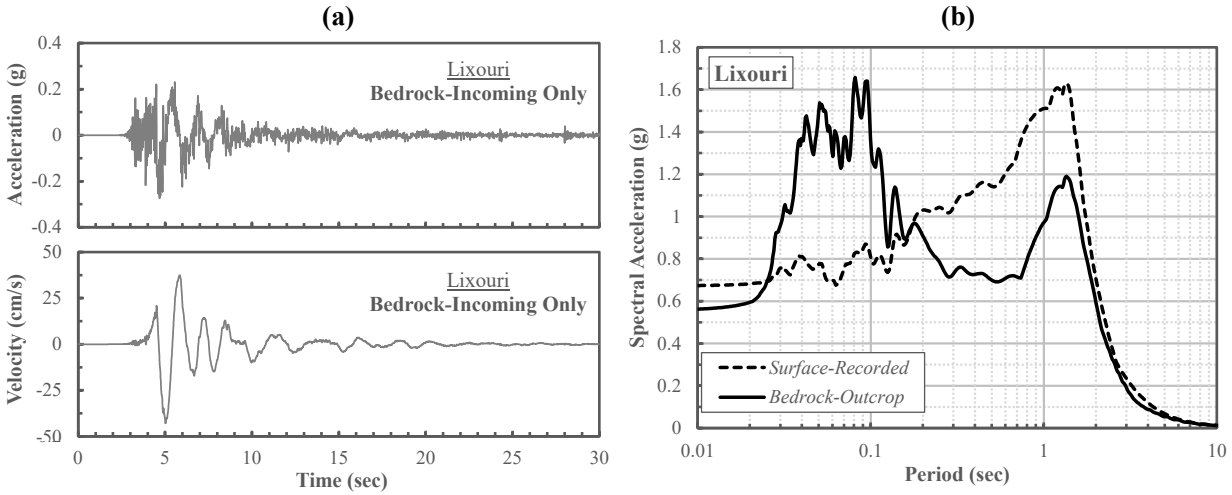

Figure 5. Deconvolution results at Lixouri: a) incoming-only, bedrock acceleration and velocity time histories, and b) bedrock outcrop and surface acceleration response spectra.

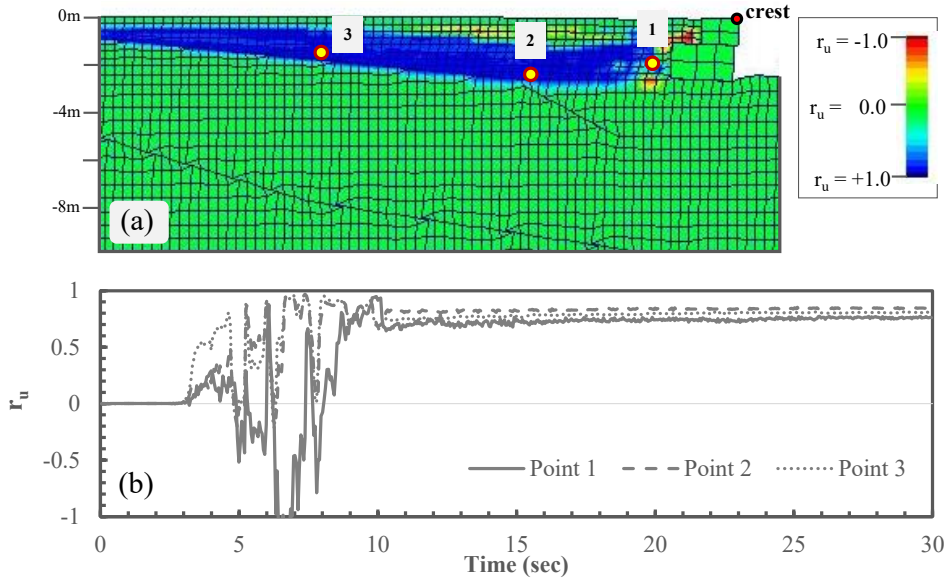

Figure 6. Computed r_u values at the Lixouri TS-7 quay wall, for PM4Sand and Best-Estimate Parameters: a) r_u contour at the end of earthquake shaking, and b) r_u time histories at three selected zones behind the quay wall.

Figure 7 illustrates the displacement and rotation time histories, as recorded at the crest of the concrete quay wall. The computed maximum displacements for the Lixouri TS-7 wall are approximately U_x=67 cm, in the seaward horizontal direction, and U_y=14 cm, in the downward vertical direction (Figure 7a), while the maximum wall rotation reached 2.5 degrees (Figure 7b). Figure 7c illustrates a comparison of the numerical results between PM4Sand, UBCSand and the URS/ROTH model, using the best-estimate parameters (Table 2). The computed wall crest displacements are similar between the PM4Sand and UBCSand models, with differences on the order of less than 10%. On the other hand, URS/ROTH results in approximately 1.5 times larger horizontal displacements of the TS-7 wall than both PM4Sand and UBCSand models. This difference can be partially attributed to the fact that the URS/ROTH model assigns residual shear strength parameters once liquefaction is triggered. Therefore, the reclamation fill material softens once liquefaction is triggered, resulting in substantially larger deformations.

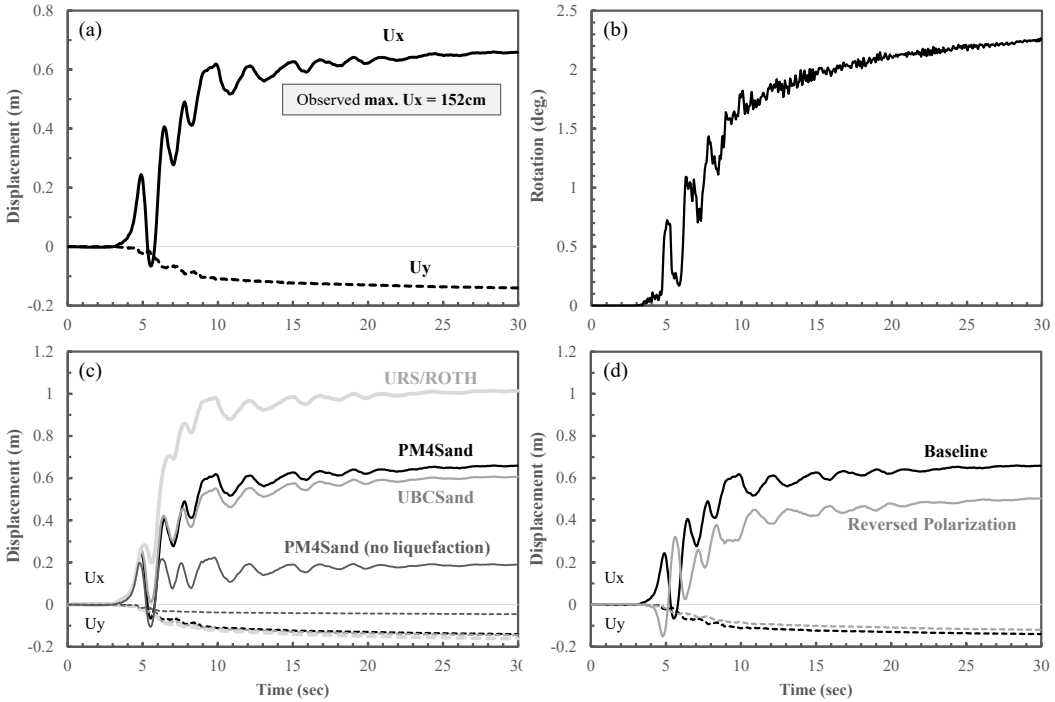

Figure 7. Computed time histories at the crest of the Lixouri TS-7 quay wall: a) horizontal and vertical displacements (PM4Sand), b) rotation (PM4Sand), c) PM4Sand, UBCSand, and URS/ROTH model comparison, and d) effect of input motion polarization (PM4Sand).

To evaluate the contribution of liquefaction occurrence on the estimated wall crest movements, additional numerical analysis was performed using the PM4Sand model with no liquefaction triggering, i.e., assuming a fictitious relative density of D_R=80% for the reclamation fill that did not allow for pore pressure generation. Based on the numerical results (Figure 7c), the contribution of liquefaction of the earthfill to the total lateral deformation of the quay walls is significant for the TS-7 wall; when liquefaction is not triggered, the computed horizontal displacements are only 30% of the displacements when liquefaction is triggered. Figure 7 also illustrates the effect of the input motion characteristics on the system response. More specifically, the displacement time histories for the Lixouri TS-7 quay wall show a pronounced

step-like form, particularly at t=5-8 sec (Figure 7a), which coincides with the pulse-like characteristic of the input velocity time series (Figure 5a), something that indicates a pronounced effect of forward rupture directivity. The influence of forward rupture directivity on the response of the TS-7 wall is also validated by performing the baseline analysis (PM4Sand) using a reversed polarization of the input motion (Figure 7d). In that case, the ultimate maximum displacements are reduced by about 25%.

Finally, when compared to the observed response, all best-estimate numerical models for the TS-7 wall seem to underpredict the field displacements (max U_x=152 cm, Figure 2b). Incorporating residual strength parameters (URS/ROTH) once liquefaction is triggered seems to reduce the discrepancy between the observed and baseline-computed responses. Nevertheless, it should be noted that, other softening mechanisms which cannot be directly captured by the used constitutive models may have contributed to the system response. Such softening mechanisms could be attributed to: a) the multidirectional nature of the actual seismic loading (e.g. Pyke et al. 1975), and b) the inability of the used constitutive models to adequately simulate the post-liquefaction soil behavior (Gerolymos et al., 2019).

CONCLUSIONS

Informed by recorded strong ground motions (Figure 2), observations from post-event reconnaissance deployments (Athanasopoulos et al., 2019) (Figure 2), and data from several in-situ investigations (Figure 3), numerical simulations of the seismic response of a selected Lixouri port quay wall system were performed. Three advanced constitutive frameworks were utilized for the simulation of the liquefiable reclamation fills (PM4Sand, UBCSand, and URS/ROTH).

Based on the simulations, it was observed that PM4Sand and UBCSand models seem to yield very similar deformational results. Moreover, it was shown that liquefaction of the gravelly earthfills increased the quay wall lateral displacements by 2.5 times, while forward rupture directivity in Lixouri was estimated to contribute 25% of the total horizontal deformations (Figures 7d). It was also observed that the URS/ROTH model produces 1.5 times greater horizontal deflections than the PM4Sand and UBCSand models, something that is attributed to the incorporation of residual shear strength parameters once liquefaction is triggered. Compared to the field measurements (Figure 2b), all numerical models underpredicted the observed horizontal displacements at the selected location.

ACKNOWLEDGEMENTS

Partial funding for this study was provided by the National Science Foundation CMMI Grants No. 1663288. Any opinions, findings, and conclusions or recommendations expressed in this material are those of the authors and do not necessarily reflect the views of the National Science Foundation.

REFERENCES

Athanasopoulos, G. A. (1995). “Empirical correlations vs-NSPT for soils of Greece: a comparative study of reliability,” In *Proceedings of 7th international conference on soil dynamics and earthquake engineering, Chania, Crete*. Southampton: Computational Mechanics, p. 19–36.

Athanasopoulos, G. A., G. C. Kechagias, D. Zekkos, A. Battilas, X. Karatzia, F. Lyrantzaki, and A. Platis. (2019). "Lateral spreading of ports in the 2014 Cephalonia, Greece, earthquakes," *Soil Dynamics and Earthquake Engineering*, 128, 105874.

Athanasopoulos-Zekkos, A., D. Zekkos, K. M. Rollins, J. Hubler, J. Higbee, and A. Platis. (2019). "Earthquake Performance and Characterization of Gravel-Size Earthfills in the Ports of Cephalonia, Greece, following the 2014 Earthquakes," in *7th International Conference on Earthquake Geotechnical Engineering*, Rome, Italy.

Beaty, M. H., and P. M. Byrne. (2011). "UBCSAND constitutive model version 904aR," Documentation Report: UBCSAND Constitutive Model on Itasca UDM Web Site, 69.

Boulanger, R. W., and I. M. Idriss. (2011). "Cyclic failure and liquefaction: Current issues," *5th Int. Conference on Earthquake Geotechnical Engineering*, Santiago, Chile, Jan 10-13.

Boulanger, R. W., and K. Ziotopoulou. (2018). "PM4Sand (Version 3.1): A sand plasticity model for earthquake engineering applications," Report No. UCD/CGM-17/01, Center for Geotechnical Modeling, University of California, Davis, CA, 2018, p. 109.

Cao, Z., T. L. Youd, and X. Yuan. (2013). "Chinese dynamic penetration test for liquefaction evaluation in gravelly soils," *Journal of Geotechnical and Geoenvironmental Engineering*, 139(8), 1320–1333.

Dawson, E. M., W. H. Roth, S. Nesarajah, G. Bureau, and C. A. Davis. (2001). "A practice oriented pore pressure generation model," *2nd FLAC Symposium on Numerical Modeling in Geomechanics*, Lyon, France.

Garini, E., G. Gazetas, and I. Anastasopoulos. (2017). "Evidence of significant forward rupture directivity aggravated by soil response in an Mw6 earthquake and the effects on monuments," *Earthquake Engineering & Structural Dynamics*, 46(13), 2103-2120.

GEER/EERI/ATC. (2014). *Earthquake reconnaissance January 26th/February 2nd 2014 Cephalonia, Greece events*, Version 1: June 6. 2014.

Geoconsult Ltd. (2016). "Geotechnical report on the assessment of the geotechnical investigation at the port of Argostoli following the Cephalonia earthquakes of January 26 and February 3rd 2014," (in Greek).

Gerolymos, N., M. Anthi, and K. Argyroulis. (2019). "Seismic effective stress analysis of caisson-type quay walls: A comparative study between constitutive models," in *7th International Conference on Earthquake Geotechnical Engineering*, Rome, Italy, 17-20 June 2019.

Idriss, I. M., and R. W. Boulanger. (2008). "Soil liquefaction during earthquakes," Monograph MNO-12, Earthquake Engineering Research Institute, Oakland, CA, 261.

Itasca. (2016). *FLAC – Fast Lagrangian Analysis of Continua, Version 8.0*, Itasca Consulting Group, Inc., Minneapolis, Minnesota.

Pyke, R., B. Seed, and C. Chan. (1975). "Settlement of sand under multidirectional shaking," *Journal of the Geotechnical Journal Division*, 101(4), 379-398.

Talbot, M. H. (2018). *Dynamic Cone Penetration Tests for Liquefaction Evaluation of Gravelly Soils*, Brigham Young University, Theses and Dissertations 7542, https://scholarsarchive.byu.edu/etd/7542.